Received: 3 February 2020 | Revised: 10 April 2020 | Accepted: 12 April 2020

DOI: 10.1002/aoc.5758

Applied Organometallic Chemistry WILEY

FULL PAPER

The influence of ultrasonic irradiation on catalytic performance of ZnO nanoparticles toward the synthesis of chiral 1-substituted-1*H*-tetrazolederivatives from *α*-amino acid ethyl esters

Yasser Mahmoud A. Mohamed[1] | **Yasser A. Attia**[2]

[1]Photochemistry Department, National Research Center, Dokki, Giza, 12622, Egypt

[2]National Institute of Laser Enhanced Sciences, Cairo University, Giza, 12613, Egypt

Correspondence
Yasser Mahmoud A. Mohamed, Photochemistry Department, National Research Center, Dokki, Giza 12622, Egypt.
Email: y.m.a.mohamed@outlook.com

Yasser A. Attia, National Institute of Laser Enhanced Sciences, Cairo University, Giza, 12613, Egypt.
Email: yasserniles@niles.edu.eg

Abstract

In this work, a simple and greener protocol for the synthesis of 1-substituted 1*H*-tetrazole derived from *α*-amino acid ethyl esters was demonstrated in the presence of zinc oxide nanoparticles (ZnO NPs) under conventional conditions, with heating (at 60 and 80°C and under reflux) compared with ultrasonic. The effect of solvent was investigated to reveal that the solvent system CH_3CN/H_2O was optimum to obtain 1-substituted 1*H*-tetrazole in high yield. In addition, the effect of irradiation power was studied, which showed that the yield of the reaction was improved at 200 W and the reaction time was shortened to be 30 min. Also, an improvement in the rate of the reaction and the yield of the products was observed when reactions were carried out under sonication conditions in the presence of ZnO NPs compared with conventional methods using various zinc salts as catalysts. The yields of tetrazole compounds **2a–i** under sonication were determined (88–96%). Furthermore, the investigated heterogeneous catalytic system was recycled and reused for five runs with significant production of tetrazole **2a** as a model target compound in excellent yields at each reaction cycle. In general, the investigated synthetic strategy for the heterocyclization of *α*-amino acid ethyl ester derivatives to 1-substituted 1*H*-tetrazoles was in agreement with the green chemistry point of view.

KEYWORDS

nanocatalysts, tetrazoles, ultrasonic-assisted, ZnO NPs, *α* -amino acid ethyl esters

1 | INTRODUCTION

The sonochemical approach in the synthesis of heterocyclic rings has received significant attention in recent years.[1,2] The strategy of ultrasound offers many advantages to promote the design and development of sensitive molecules and it has also assisted in obtaining the products in high yields and selectivity.[3,4] In recent years, several studies have reported that the sonication of multicomponent reactions can lead to accelerated reaction rates via the formation and adiabatic collapse of transient cavitation bubbles. The ultrasonic effect induces very high local pressure and temperatures inside the bubbles and enhances mass transfer and turbulent flow in the liquid.[5–8] Another important factor that affects the results of chemical reactions is the use of heterogeneous

catalysts that could offer many advantages from both economic and environmental points of view.[9] ZnO nanoparticles have been considered one of the most promising nanocatalysts because of their wide band-gap energy, physical and chemical stability, high oxidative capacity, low cost and ease of availability.[10,11] As a continuation of our previous work on the development of heterogeneous catalytic systems for the synthesis of beneficial organic compounds,[12–16] we aimed in this study to synthesize a series of 1-substituted-1*H*-tetrazoles derived from some α-amino acid ethyl ester derivatives through the utility of zinc oxide nanoparticles (ZnO NPs) as an efficient nanocatalyst under sonication conditions. Currently, scientists are seeking to develop new methods for the synthesis of tetrazole and its derivatives through facile, eco-friendly and low-cost approaches to testing these tetrazoles in applications. Hence, new synthetic approaches for the rational design of polyfunctional materials based on a tetrazole nucleus to improve the classical procedures for the preparation of tetrazole derivatives have been reported in various studies.[17–21] Tetrazoles were first synthesized the heterocycle in 1885 through the reaction of hydrazoic acid and hydrogen cyanide under pressure.[22] In 1961, the Ugi-azide procedure was developed, which yielded 1,5-disubstituted tetrazole derivatives through a multicomponent reaction.[23] A relatively simple synthetic method for the preparation of 1-substituted tetrazoles was developed in 1973 that included the heterocyclization reaction of primary amines and their salts with orthoesters and sodium azide in the presence of acetic acid[24] (Scheme 1).

Afterward this, research on the synthesis of tetrazole compounds began to develop rapidly and tetrazole derivatives have attracted interest.[25–29] Few reports on the application of heterogeneous catalysts in the direct synthesis of 1-substituted-1*H*-tetrazoles have been described in the literature,[30–32] although there are some studies related to the preparation of 1-substituted-1*H*-tetrazoles from amines using various conditions, especially using heterogeneous nanocatalysts.[33–38] Hence, the development of efficient heterogeneous catalytic systems for the promotion of the cyclization of primary amines to tetrazoles is much needed.

2 | EXPERIMENTAL

2.1 | Materials and methods

All chemicals were obtained from Sigma-Aldrich and used without further purification. Thin-layer chromatography was performed using silica gel plates (60 GF254) and cellulose plates (20 × 20 cm). The infrared spectra were recorded as a thin film on a PerkinElmer Fourier transform infrared (FTIR) spectrometer. The nuclear magnetic resonance (NMR) spectra were obtained on a Bruker Avance DPX (300 MHz for ^{1}H and 75 MHz for and ^{13}C). The chemical shift data are reported in parts

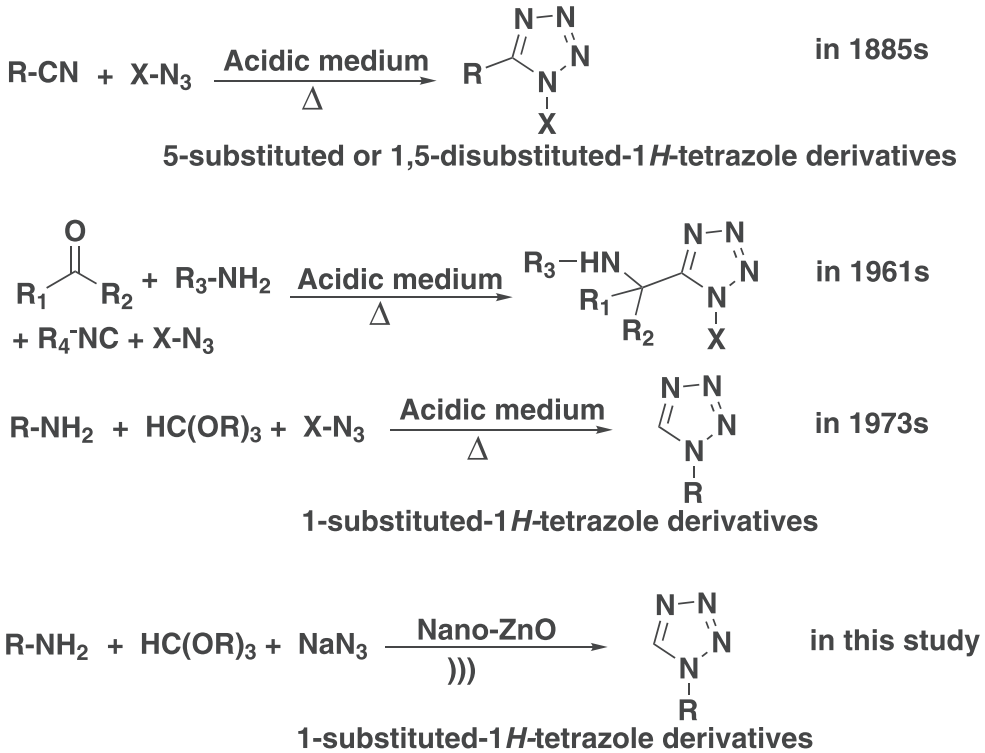

SCHEME 1 Synthetic strategies in the synthesis of tetrazoles

per million (ppm) downfield from tetramethylsilane. DMSO-d_6 was as a partially deuterated-NMR solvent. High-resolution mass spectrometry (HRMS) analysis was performed using a 6230 series accurate-masstime-of-flight liquid chromatography (LC)/MS system. To resolve the enantiomers, an LC/MS-compatible mobile phase system was used on an Astec Chirobiotic® T column. UV–vis spectra were recorded on a Hewlett-Packard 8452A diode-array spectrophotometer. X-ray diffraction (XRD) measurements were performed using a Philips PW1710 X-ray diffractometer using Cu Kα radiation (k = 1.54186 Å). The XRD patterns were recorded from 20 to 70° 2H, with a step size of 0.020° 2H and collecting 10 s per step. Transmission electron microscopy (TEM) micrographs of the colloidal particles were measured using a Jeol JEM-2100 of 200 kV with a magnification range of 1000× to 50,000×. The TEM samples were prepared and placed on a copper grid by mixing one dilute drop of prepared aqueous particles dispersed in 5 ml acetone to produce a slightly turbid solution that was allowed to dry thoroughly. Scanning electron microscopy (SEM) images were obtained with a Zeiss FE-SEM ULTRA Plus (equipped with an EDX analyzer) microscope with a Philips CM20 microscope, operating at an accelerating voltage of 200 kV. Several drops from the sample dispersion were deposited onto an aluminum pin stub and left to evaporate at room temperature.

2.2 | Synthesis of ZnO nanoparticles[39]

Zinc oxide nanoparticles were prepared by a chemical reduction of zinc precursor, using ascorbic acid, trisodium citrate and NaOH. Briefly, 100 ml deionized water containing 50 mM trisodium citrate and 4 mM ascorbic acid was brought to boiling under stirring conditions. To this solution, 3 ml of 2.5 M zinc sulfate solution was added drop-wise at the rate of 0.2 ml/min. The color of the solution changed from pale to bright white. By the addition of 1.0 ml of 2 M NaOH solution, the color changed to white, indicating the onset of ZnO NP synthesis. The ZnO NP suspension was centrifuged at 9000 rpm for 15 min followed by washing of the pellet two or three times with Milli-Q water.

2.3 | Synthesis of tetrazole derivatives

2.3.1 | Optimized reaction conditions

To a mixture of appropriate α-amino acid ethyl ester hydrochloride salts (1.0 mmol) and ZnO NPs (5 wt%) in CH_3CN (3 ml) and H_2O (3 ml), was added solid NaN_3 (1.5 mmol) and triethyl orthoformate (1.0 mmol). The reaction mixture was performed under the following conditions: (a) stirred at room temperature for 24 h; (b) stirred at different temperatures—60 and 80°C—and under reflux conditions for 24 h; and (c) subjected to sonication using a multiwave ultrasonic generator operating at 20 kHz with a maximum power output of 200 W for 30 min. The reaction was monitored by thin-layer chromatography. The reaction mixture was extracted with ethyl acetate (3 × 15 ml). Under vacuum, the combined organic layers were dried over sodium sulfate, filtered and concentrated. The residue was purified using cold crystallization (ethyl acetate/hexanes) to afford tetrazole compounds **2a–i** in excellent yields.

2.3.2 | Ethyl 2-(1*H*-tetrazol-1-yl)acetate (2a)

^{1}H NMR (300 MHz, DMSO-d_6) δ (ppm): 1.33 (t, 3H, J = 6.8 Hz), 3.56 (q, 2H, J = 6.8 Hz), 4.12 (s, 2H), 8.09 (s, 1H tetrazole); ^{13}C NMR (75 MHz, DMSO-d_6) δ (ppm): 14.0, 52.7, 62.9, 148.8, 172.9; m/z (HRMS): calcd for $C_5H_8N_4O_2$: 156.0647; found: 157.1071 $[M + H]^+$.

2.3.3 | *(R)*-Ethyl2-(1*H*-tetrazol-1-yl) propanoate (2b)

^{1}H NMR (300 MHz, DMSO-d_6) δ (ppm): 1.29 (t, 3H, J = 6.8 Hz, CH_3), 2.55 (d, 3H, J = 5.6 Hz, CH_3), 3.54 (q, 1H, J = 5.6 Hz, CH), 4.11 (q, 2H, CH_2, J = 6.8 Hz), 8.11 (s, 1H tetrazole); ^{13}C NMR (75 MHz, DMSO-d_6) δ (ppm): 14.1, 14.3, 54.5, 61.9, 146.6, 176.4; m/z (HRMS): calcd for $C_6H_{10}N_4O_2$: 170.0804; found: 171.0974 $[M + H]^+$.

2.3.4 | *(R)*-Ethyl-3-methyl-2-(1*H*-tetrazol-1-yl)butanoate (2c)

^{1}H NMR (300 MHz, DMSO-d_6) δ (ppm): 1.09 (m, 6H, $2CH_3$), 1.42 (t, 3H, J = 6.8 Hz, CH_3), 2.64–2.76 (m, 1H, CH), 4.18 (q, 2H, J = 6.8 Hz), 4.92 (t, 1H, J = 4.2 Hz, CH), 8.24 (s, 1H tetrazole); ^{13}C NMR (75 MHz, DMSO-d_6) δ (ppm): 13.6, 18.7, 20.3, 24.5, 69.7, 145.1, 175.7; m/z (HRMS): calcd for $C_8H_{14}N4O_2$: 198.1116; found: 199.1209 $[M + H]^+$.

2.3.5 | *(R)*-4-Methyl-2-(1*H*-tetrazol-1-yl) pentanoic acid (2d)

^{1}H NMR (300 MHz, DMSO-d_6) δ (ppm): 0.87–1.01 (m, 6H, $2CH_3$), 1.46 (t, 3H, J = 6.8 Hz, CH_3), 1.82–2.03 (m,

1H, CH), 4.17 (q, 2H, J = 6.8 Hz), 4.88 (t, 1H, J = 4.2 Hz, CH), 8.66 (s, 1H tetrazole); ^{13}C NMR (75 MHz, DMSO-d_6) δ (ppm): 13.6, 21.4, 24.0, 25.8, 42.7, 67.1, 144.7, 176.1; m/z (HRMS): calcd for $C_9H_{16}N_4O_2$: 212.1273; found: 213.1197 $[M + H]^+$.

2.3.6 | *(R)*-ethyl 3-hydroxy-2-(1*H*-tetrazol-1-yl)propanoate (2e)

^{1}H NMR (300 MHz, DMSO-d_6) δ (ppm): 1.27 (t, 3H, J = 6.8 Hz, CH_3), 2.37 (br, s, 1H, OH), 3.65 (q, 2H, J = 6.8 Hz), 3.91 (d, J = 4.2 Hz, 2H, CH_2), 4.62 (t, 1H, J = 4.2 Hz, CH), 8.21 (s, 1H tetrazole); ^{13}C NMR (75 MHz, DMSO-d_6) δ (ppm): 13.6, 44.3, 53.2, 60.7, 148.5, 176.8; m/z (HRMS): calcd for $C_6H_{10}N_4O_3$: 186.1710; found: 187.2023 $[M + H]^+$.

2.3.7 | *(R)*-ethyl 3-phenyl-2-(1*H*-tetrazol-1-yl)propanoate (2f)

^{1}H NMR (300 MHz, DMSO-d_6) δ (ppm): 1.39 (t, 3H, J = 6.8 Hz, CH_3), 3.25 (d, J = 4.2 Hz, 2H, CH_2), 4.18 (q, 2H, J = 6.8 Hz, CH_2), 4.61 (t, J = 4.2 Hz, 1H, CH), 7.29–7.56 (m, 5H), 8.19 (s, 1H tetrazole); ^{13}C NMR (75 MHz, DMSO-d_6) δ (ppm): 13.9, 44.3, 53.4, 60.9, 127.6, 128.9, 129.8, 131.9, 146.4, 143.5, 175.6; m/z (HRMS): calcd for $C_{12}H_{14}N_4O_2$: 246.1117; found: 247.1610 $[M + H]^+$.

2.3.8 | *(R)*-ethyl 3-(4-hydroxyphenyl)-2-(1*H*-tetrazol-1-yl)propanoate (2g)

^{1}H NMR (300 MHz, DMSO-d_6) δ (ppm): 1.32 (t, 3H, J = 6.8 Hz, CH_3), 3.14 (d, J = 4.2 Hz, 2H, CH_2), 4.11 (q, 2H, J = 6.8 Hz), 4.72 (t, J = 4.2 Hz, 1H, CH), 5.64 (br, s, 1H, OH), 7.21–7.53 (m, 4H), 8.14 (s, 1H tetrazole); ^{13}C NMR (75 MHz, DMSO-d_6) δ (ppm): 14.1, 46.3, 54.5, 61.6, 128.6, 129.3, 134.5, 146.23, 155.2, 177.6; m/z (HRMS): calcd for $C_{12}H_{14}N_4O_3$: 262.1066; found: 263.1185 $[M + H]^+$.

2.3.9 | *(R)*-ethyl 3-(1*H*-imidazol-4-yl)-2-(1*H*-tetrazol-1-yl)propanoate (2h)

^{1}H NMR (300 MHz, DMSO-d_6) δ (ppm): 1.39 (t, 3H, J = 6.8 Hz, CH_3), 3.39–3.43 (m, 2H, CH_2), 4.16 (q, 2H, J = 6.8 Hz), 4.91 (dd, J = 4.2 Hz, 1H, CH), 5.11 (br, s, 1H, NH), 6.35 (s, 1H, imidazole ring), 7.39 (s, 1H imidazole), 8.36 (s, 1H tetrazole); ^{13}C NMR (75 MHz, DMSO-d_6) δ (ppm): 13.8, 30.6, 64.7, 116.8, 133.6, 134.5, 145.2, 176.8; m/z (HRMS): calcd for $C_9H_{12}N_6O_2$: 236.1022; found: 236.1274 $[M + H]^+$.

2.3.10 | *(R)*-3-(1*H*-indol-3-yl)-2-(1*H*-tetrazol-yl)propanoic acid (2i)

^{1}H NMR (300 MHz, DMSO-d_6) δ (ppm): 1.39 (t, 3H, J = 6.8 Hz, CH_3), 3.72–3.87 (m, 2H, CH_2), 4.16 (q, 2H, J = 6.8 Hz), 4.97 (dd, J = 4.2 Hz, 1H, CH), 6.81–6.94 (m, 4H, indole ring), 7.29–7.43 (m, 1H, indole), 8.64 (s, 1H tetrazole), 10.16 (br, s, 1H, NH); ^{13}C NMR (75 MHz, DMSO-d6) δ (ppm): 13.8, 28.7, 62.8, 109.2, 111.8, 116.1, 118.4, 121.3, 122.9, 126.3, 136.5, 144.3, 175.2; m/z (HRMS): calcd for $C_{14}H_{15}N_5O_2$: 285.1266; found: 286.1502 $[M + H]^+$.

2.4 | Catalyst recyclability

After completion of the reaction, the mixture was diluted by H_2O–EtOAc (v/v, 1:1, 10 ml), stirred at ambient temperature (20 min) and filtered to collect the catalyst. The solid catalyst was dried at room temperature under reduced pressure to obtain almost quantitatively ZnO nanoparticles.

3 | RESULTS AND DISCUSSION

3.1 | Catalyst preparation and characterization

The TEM image of ZnO NPs is depicted in Figure 1. It was observed that ZnO NPs have a spherical structure with a mean diameter ranging from 35 to 44 nm (Figure 1a). SEM images with the mapping of the ZnO NPs are shown in Figure 1b–d, confirming the results from the TEM image. The chemical composition of ZnO NPs was analyzed by energy dispersive spectrometry on an SEM (Figure 1e). The result shows the peaks of O, and Zn at 28.42 and 72.58 wt%, respectively, confirming that the sample is of high purity.

The UV–vis spectrum of the prepared ZnO NPs is shown in Figure 2a. It is clear that ZnO NPs are semiconductors with a wide bandgap (3.3 eV) that makes them a suitable absorber of UV radiation exhibiting a sharp band at 375 nm.[14] The XRD pattern of the as-prepared ZnO NPs is depicted in Figure 2b. The diffraction peaks are quite similar to those of bulk ZnO, which can be indexed as the hexagonal wurtzite structure ZnO (a = 3.249 Å, c = 5.206 Å) and diffraction data were in

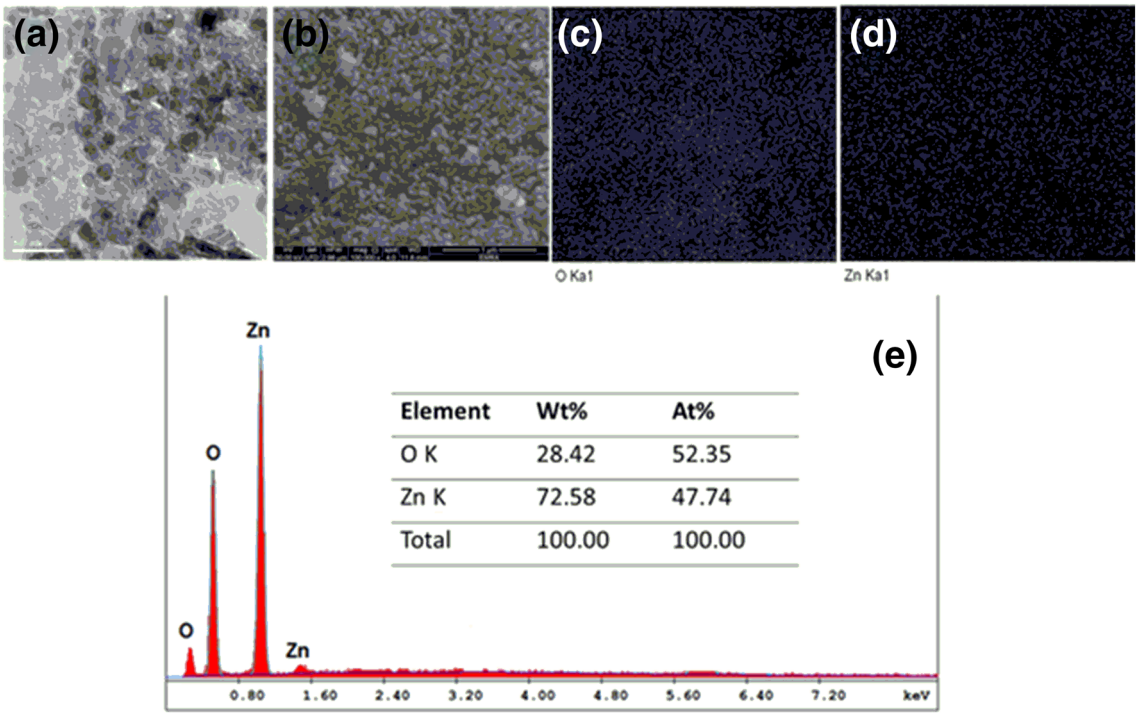

FIGURE 1 Transmission electron microscopy image of the synthesized zinc oxide nanoparticles (ZnO NPs) (a) and scanning electron microscopy images of ZnO NPs (b–d) with energy dispersive spectrometry analysis of ZnO NPs (e)

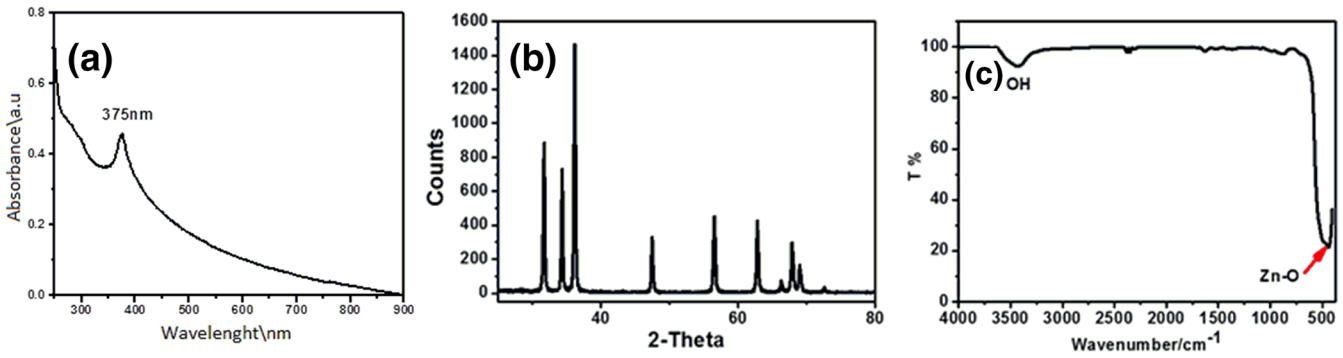

FIGURE 2 Absorption spectrum (a), X-ray diffraction pattern (b) and Fourier transform infrared spectrum (c) of ZnO nanoparticles

agreement with the JCPDS card for ZnO (JCPDS 36-1451). No other peaks were detected, implying that the prepared nanostructure materials are pure ZnO.[40] The XRD pattern of the as-prepared ZnO NPs is shown in Figure 2b and shows the presence of wurtzite ZnO owing to presence of three distinct features: the first at $2\theta = 36.252^{\circ}$ is due to (101) reflection of planes and $2\theta = 34.440^{\circ}$ and 56.555° are due to (200) and (011) reflection of planes, respectively. The FTIR spectrum of ZnO NPs was recorded in the range 390–4000 cm^{-1} (Figure 2c). A significant vibration band ranging from 400 to 500 cm^{-1} was assigned to the characteristic stretching mode of the Zn–O bond. The broad peak 3434 cm^{-1} (stretching) indicates the presence of hydroxyl groups of absorbed H_2O molecules.

3.2 | Catalytic performance of ZnO NPs towards the synthesis of 1-substituted-1*H*-tetrazole derivatives from *α*-amino acid ethyl esters

Various parameters were studied, such as solvent system, irradiation power, catalyst loading and irradiation time, and a comparison was made between the catalytic activity of ZnO NPs and other Zn precursors to obtain the

optimum reaction conditions for heterocyclization of some of α-amino acid ethyl esters to their corresponding tetrazoles.

3.2.1 | Effect of solvent and temperature on the synthesis of tetrazoles

The initial step of this synthetic protocol was started by exploring optimized reaction conditions. In the first series of experiments, our effort was focused on determining an appropriate solvent for performing the reaction. Thus, the reaction of glycine ethyl ester (**1a**) with triethyl orthoformate [HC $(OEt)_3$] and sodium azide (NaN_3) in the presence of ZnO NPs (1 wt%) was selected as a model reaction. Initially, the effect of different solvents under three different reaction conditions—room temperature, heating and sonication—was screened for preparation of the corresponding ethyl 2-(1*H*-tetrazol-1-yl)acetate (**2a**) (Scheme 2 and Table 1).

In this protocol, when the model reaction was employed under solvent-free conditions after 24 h at room temperature and at 100°C, or even if the reaction was performed under sonication conditions for 8 h, the reaction was not conducted (entry 1). It was also found that the solvents like DMF, THF, EtOH and H_2O were inappropriate for the progress of this reaction (Table 1, entries 3–6). As observed in Table 1, different solvents were used under various conditions. However, the highest yield of product **2a** was obtained in 76 and 87%, respectively, when the CH_3CN and CH_3CN–H_2O solvents were used under ultrasound irradiation (entry 7). The reaction temperature was taken into account during the progress of the reaction. It was demonstrated that compound **2a** was obtained in low to moderate yields when the reaction was performed at room temperature or under elevated temperatures (60 and 80°C and under reflux condition) (Table 1, entries 2–7). This indicated that the increase in the reaction temperature had no distinguishable effect on the progress of the model reaction. However, the yield of 1H-tetrazole (**2a**) was dramatically improved when CH_3CN/H_2O solvent was used under the sonication conditions. This enhancement of the reaction yield resulted because the dielectric constant of CH_3CN was 38.8[41] and the dielectric constant of water is 78.4 at 25°C.[42] Hence, the CH_3CN/H_2O system could be affected in the acceleration of longitudinal ultrasonic waves and consequently the ZnO nanoparticles, in contrast to the other solvents used in this protocol that could attenuate these waves.[43]

3.2.2 | The influence of ultrasound irradiation powers on progress of the reaction

The effect of the ultrasound power irradiation on the yield of the product **2a** was investigated by performing the reaction at different irradiation powers from 0 to 200 W at 20 kHz. It was demonstrated that, as seen from Table 2, the increase in ultrasonic power to 200 W led to a relatively higher yield (90%) at a shorter reaction time (60 min). From these results, it was indicated that the rate of the reaction increased when the irradiation power increased.

3.2.3 | Effect of catalyst loading

To investigate the ideal conditions, the effect of ZnO NPs loading at irradiation power 200 W was studied (Table 3).

In Table 3, it is shown that the yield of product **2a** was dramatically improved. The increase in the catalyst loading to 7 wt% (Table 3, entry 6) led to the same yield as obtained in the case of catalyst loading (5 wt%). This indicated that the best yield of product **2a** was obtained when the amount of catalyst was 5 wt% (Table 3, entry 5). The results indicated that merging between ultrasound irradiation method and ZnO nanoatalyst method ameliorates the product yield and reaction time.

3.2.4 | Investigation of the relationship between the irradiation time and the yield of the product

The effect of sonication time on the yield of the product **2a** was also investigated by carrying out six experiments in which the reaction mixture was exposed to ultrasound irradiation for appropriate times (0, 5, 10, 15, 20, 25 and 30 min). These experiments revealed that the increase in irradiation time led to a relatively higher yield (Table 4).

A possible explanation for the positive association between yield and time of ultrasound irradiation is that the increase in the exposure time could increase the yield of the product. In other words, the number of active

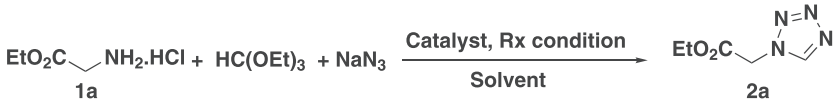

SCHEME 2 Model reaction

TABLE 1 Effect of solvents under room temperature, heating method or sonication conditions (75 W) on the synthesis of ethyl 2-(1*H*-tetrazol-1-yl)acetate (**2a**) from glycine ethyl ester (**1a**)[a] zinc oxide nanoparticles (ZnO NPs) as a catalyst

		Reaction conditions		
Entry	Solvent	Room temperature, time (h)/ yield (%)[c]	Heating method, *T* (°C)/time (h)/ yield (%)[c]	Sonication, time (h)/yield (%)[c]
1	Solvent free[b]	24/NR[d]	100/24/NR	8/NR
2	CH_3CN	24/18	60/24/39 80/24/43 reflux/24/52	8/76
3	DMF	24/traces[e]	60/24/traces 80/24/27 Reflux/24/28	8/45
4	THF	24/12	60/24/38 Reflux/24/40	8/43
5	EtOH	24/NR	60/24/19 Reflux/24/22	8/25
6	H_2O	24/NR	60/24/26 80/24/26 Reflux/24/28	8/34
7	CH_3CN/ H_2O	24/39	60/24/69 80/24/74 reflux/24/83	8/87

DMF; dimethylformamide, THF; tetrahedrofuran, EtOH; ethanol.
[a]Reaction conditions: α-amino acid ethyl ester, 1 mmol; sodim azide, 1.5 mmol; $HC(OEt)_3$, 1 mmol; ZnO NPs, 1 wt%; solvent, 6 ml.
[b]The reaction was tested in a sealed tube.
[c]Isolated yield.
[d]No reaction.
[e]Trace = the yield of the product was <10%.

TABLE 2 The effect of ultrasonic irradiation power on the synthesis of **2a** using ZnO NPs (1 wt%) and CH_3CN/H_2O solvent

Power (W)	0	75	150	200
Yield (%)[a]	0	87	88	90
Time (min)	480	480	120	60

[a]Isolated yields.

cavitation bubbles and the size of the individual bubbles are both expected to result in higher maximum collapse temperature and accelerated respective reaction[21] (Figure 3).

3.2.5 | Catalytic activity of ZnO NPs vs. zinc salts

A comparison was made between our investigated methodology in this study and previously reported methods in which zinc was used as the catalyst for the synthesis of 1H-tetrazoles. Zinc chloride was used to synthesize amino-tetrazole compounds from cyanamides under ultrasound conditions at 70–80°C to afford products in 73–80% isolated yields after 15 h.[44] Also, it was reported that commercial ZnO was used in stoichiometric amounts to promote the synthesis of

TABLE 3 Effect of ZnO nanocatalyst loading under sonication conditions (200 W) in CH_3CN/H_2O solvent system

Entry	ZnO NPs loading (wt%)	Time (min)	Yield (%)[a]
1	1	60	90
2	2	60	92
3	3	45	92
4	4	45	93
5	5	30	96
6	7	30	96

[a]Isolated yields.

TABLE 4 The effect of ultrasonic irradiation (200 W) time on the synthesis of **2a** using ZnO NPs (5 wt%) and CH_3CN/H_2O solvent

Entry	Time (min)	Yield (%)[a]
1	0	0
2	5	38
3	10	45
4	15	53
5	20	76
6	25	92
7	30	96

[a]Isolated yields.

TABLE 5 A comparison between the catalytic potency of ZnO NPs with commercial ZnO and zinc salts under ultrasonic irradiation (200 W) for 30 min

Entry	Catalyst	Yield (%)[a]
1	ZnO NPs	96
2	ZnO	49
3	$ZnCl_2$	43
4	$ZnBr_2$	37
5	ZnI_2	38
6	$ZnSO_4$	36
7	Zn $(OAc)_2$	35

[a]Isolated yield.

tetrazole under conventional methods at 120°C to produce tetrazoles in 73–8% isolate yields at 2 h.[45] In our method, product formation was completely pure and solely regioselective 1-substituted-1*H*-tetrazoles from some *α*-amino acid ethyl esters were obtained without the need for chromatographic separation. Hence, a series of experiments were performed to confirm the potential catalytic activity of ZnO NPs (5 wt%) as heterogeneous nanocatalysts in comparison with commercial zinc oxide (5 wt%) (Table 5, entry 2) and different zinc salts (5 wt%) (Table 5, entries 3–7) under the optimized reaction conditions at 30 min.

Interestingly, product **2a** was obtained in 96, 49, 43, 37, 38, 36 and 35, respectively, for the use of ZnO NPs, commercial ZnO, $ZnCl_2$, $ZnBr_2$, ZnI_2, $ZnSO_4$ and Zn $(OAc)_2$ (Table 5, entries 1–7). It can be postulated that the surface of ZnO NPs can provide suitable binding sites for the reactants which has a significant role in reaction progress compared with the commercial ZnO and other zinc salts that do not possess large surface area, as in the case of ZnO NPs.

3.3 | Recyclability of ZnO nanocatalyst

Recycling of the catalyst from the reaction is one of the important benefits of green chemistry. We studied the recovery and reusability of catalyst. The reaction was carried out with glycine ethyl ester, triethyl orthoformate and sodium azide as a model reaction in the presence of ZnO NPs under optimized conditions. The reusability of catalysts was investigated and they were reused five times with a minimal loss of activity (Table 6).

3.4 | Reaction mechanism

A proposed reaction mechanistic aspect for the present work is depicted in Scheme 3. It is obvious that ZnO NPs was coupled with triethyl orthoformate (A) to produce intermediate (B). The second step was the formation of intermediate (C) through the attack of the amine group present in *α*-amino acid ethyl ester.

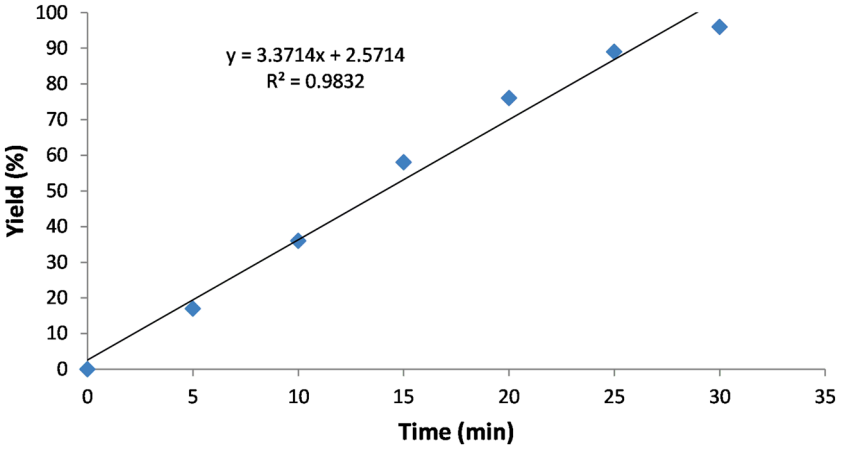

FIGURE 3 Relationship between the times of irradiation and the obtained yield of compound **2a**

TABLE 6 The reusability of ZnO NPs (5 wt%) for the synthesis of **2a** under ultrasonic irradiation (200 W)

Run no.	Yield (%)[a]
1	96
2	95
3	94
4	92
5	92

[a]Isolated yield.

Then the reaction could proceeded rapidly to produce intermediate (F), which underwent heterocyclization to yield tetrazole compound (G) (Scheme 3). This postulated mechanism was in accordance with the previous report.[46] However, this strategy facilitates synthesisis of tetrazole derivatives from α-amino acid ethyl esters under mild reaction conditions through the combination of ultrasound irradiation with ZnO nanoparticles, which has advantages from environmental and economical points of view over the reported synthetic pathway that was used for Cu nanoparticles which were produced through complex methods to perform heterocyclization of α-amino acid ethyl esters to tetrazoles at 80°C in 64–90% isolated yield at 1–7 h.[47]

Hence, the present study provided a green, simple and eco-friendly approach for the formation of 1-substituted-1*H*-tetrazoles derived from α-amino acid ethyl ester.

3.5 | Ultrasound-assisted series of 1-substituted-tetrazoles derived from α-amino acid ethyl ester derivatives

The investigated method was employed for the synthesis of other 1-substituted-tetrazoles derived from L-alanine ethyl ester (**2b**), L-valine ethyl ester (**2c**), L-leucine ethyl ester (**2d**), L-serine ethyl ester (**2e**), L-phenylalanine ethyl ester (**2f**), L-tyrosine ethyl ester (**2 g**), L-histidine ethyl ester (**2 h**) and L-tryptophan ethyl ester (**2i**) under optimum reaction conditions (catalyst, 5 wt%), as well as ethyl ester of α-amino acid (1.0 mmol) and sodium azide (1.5 mmol in MeCN/H_2O, 6.0 ml, 1:1) under ultrasound irradiation (200 W) for 30 min to obtain compounds **2b–2i** in excellent yields (Scheme 4). The yields of the obtained products are shown in Table 7. It was observed that the reactions of amino acid ethyl ester substrates were performed without loss of optical purity. The chirality was determined using chiral HPLC, which showed that the as-prepared tetrazole analogs were optically pure within limits of detection (Table 7).

As seen from the results, different substitutions on tetrazole ring could be developed through the utility of an ultrasonication procedure in the presence of recyclable ZnO nanocatalyst under the investigated optimal reaction condition. These results were in accordance with reported method in which zinc sulfide nanoparticles were used for heterocyclization of some primary amines to 1*H*-tetrazole derivatives under ultrasound.[48] It can be stated that ZnO NPs can provide heterocyclization of α-amino acid ethyl esters in a mild, clean, fast, novel and safe sonochemical procedure for synthesis of 1-substituted 1*H*-tetrazole derivatives.

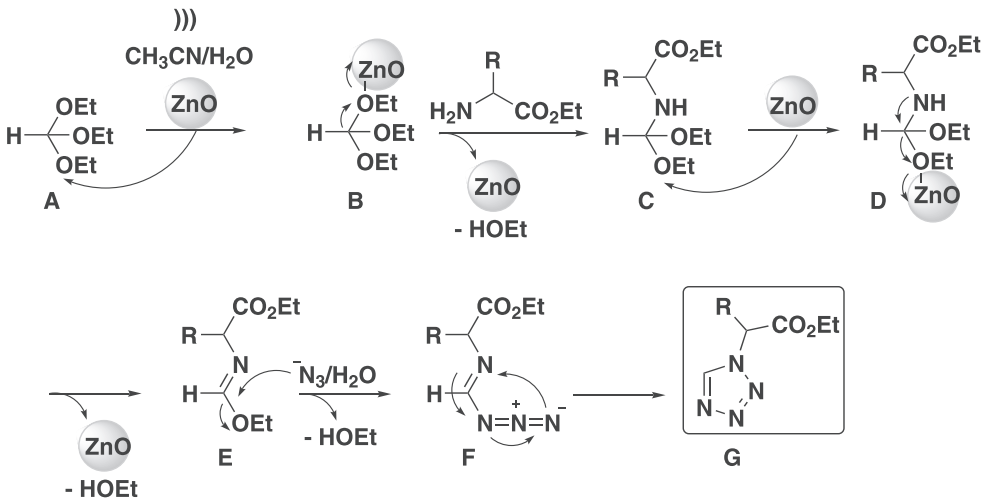

SCHEME 3 Postulated mechanism for producing tetrazoles from α-amino acid ethyl ester derivatives

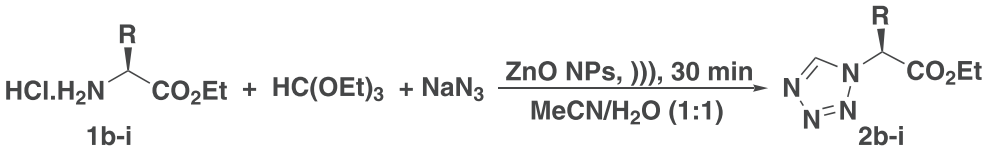

b, R= CH_3 (L-alanine ethyl ester hydrochloride)
c, R= $CH(CH_3)_2$ (L-valine ethyl ester hydrochloride)
d, R= $CH_2CH(CH_3)_2$ (L-leucine ethyl ester hydrochloride)
e, R= CH_2OH (L-serine ethyl ester hydrochloride)
f, R= CH_2Ph (L-phenyl alanine ethyl ester hydrochloride)
g, R= CH_2-C_6H_4-4-OH (L-tyrosine ethyl ester hydrochloride)
h, R= CH_2-4-imidazole (L-histidine ethyl ester hydrochloride)
i, R= CH_2-2-1*H*-indole (L-tryptophane ethyl ester hydrochloride)

SCHEME 4 Synthesis of some tetrazoles derived from some of α-amino acid ethyl ester derivatives

TABLE 7 The catalytic activity of the ZnO NPs towards the synthesis of teterazoles **2b–i** from α-amino acid ethyl esters **1b–i** under optimized reaction conditions[a]

Entry	Product	Enantiomeric ratio[b]	$[\alpha]_D^{25}$ (c = 1, MeOH)	Yield (%)[c]
1	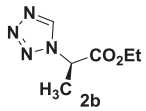 2b	16:1	+18.46	95
2	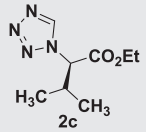 2c	19:1	+21.30	91
3	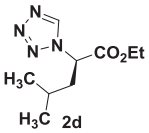 2d	16:1	+19.43	88
4	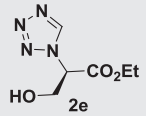 2e	25:1	+16.83	92
5	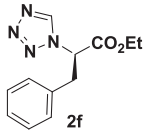 2f	25:1	+20.57	89
6		50:1	+14.17	93

TABLE 7 (Continued)

Entry	Product	Enantiomeric ratio[b]	$[\alpha]_D^{25}$ (c = 1, MeOH)	Yield (%)[c]
	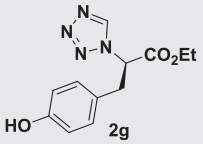 2g			
7	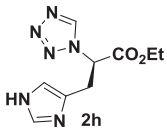 2h	25:1	+2.23	92
8	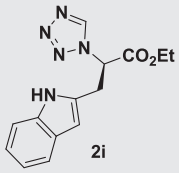 2i	19:1	+12.96	95

[a]Reagents and reaction conditions: α-amino acid ethyl esters **1b–i** (1.0 mmol), NaN_3 (1.5 mmol), HC $(OEt)_3$ (1.0 mmol), catalyst (5 wt%) under sonication for 30 min.
[b]Determined by chiral HPLC.
[c]Isolated yield.

4 | CONCLUSIONS

In this report, an efficient ultrasound-assisted and green protocol for the three-component reaction of a series of α-amino acid ethyl esters, triethyl orthoformate and sodium azide in the presence of ZnO nanocatalysts to produce chiral 1-substituted-1*H*-tetrazole analogs under optimum conditions was investigated. The main features of this approach are the use of mild reaction conditions that excluded the formation of HN_3, no production of side products, easy work-up and high yields. Recovery and reuse of the nanocatalysts were also satisfactory, which demonstrates the cost efficiency and green aspect of our methodology.

ACKNOWLEDGEMENT

The authors are grateful to the National Research Center (Egypt) and National Institute of Laser Enhanced Sciences, Cairo University (Egypt) for providing the facilities.

CONFLICT OF INTEREST

The authors have declared no conflict of interest.

FUNDING

This research did not receive any specific grant from funding agencies in the public, commercial, or not-for-profit sectors.

ORCID

Yasser Mahmoud A. Mohamed https://orcid.org/0000-0003-4678-9767
Yasser A. Attia https://orcid.org/0000-0002-5830-2250

REFERENCES

[1] J.-Y. He, H.-Z. Jia, Q.-G. Yao, S.-J. Liu, H.-K. Yue, H.-W. Yu, R.-S. Hu, *Ultrason. Sonochem.* **2015**, *22*, 144.
[2] A. Alizadeh, H. Sedighian, R. Ghanbaripour, *Helv. Chim. Acta* **2014**, *97*, 447.
[3] M. J. Lo Fiego, M. A. Badajoz, C. Domini, A. B. Chopa, M. T. Lockhart, *Ultrason. Sonochem.* **2013**, *20*, 826.
[4] S. Alaouia, M. Driowya, L. Demange, R. Benhida, K. Bougrin, *Ultrason. Sonochem.* **2018**, *40*, 289.
[5] P. D. Jolhe, B. A. Bhanvase, V. S. Patil, S. H. Sonawane, I. Potoroko, *Ultrason. Sonochem.* **2017**, *39*, 153.
[6] B. A. Bhanvase, S. H. Sonawane, *Chem. Eng. Proc.: Proc. Intensific.* **2014**, *85*, 86.
[7] B. A. Bhanvase, D. V. Pinjari, S. H. Sonawane, P. R. Gogate, A. B. Pandit, *Ultrason. Sonochem.* **2012**, *19*, 97.

[8] B. A. Bhanvase, N. S. Darda, N. C. Veerkar, A. S. Shende, S. H. Sonawane, *Ultrason. Sonochem.* **2015**, *24*, 87.
[9] V. P. Ananikov, I. P. Beletskaya, *Nanotech. Russ.* **2010**, *5*, 1.
[10] M. Abdollahi-Alibeik, A. Moaddeli, *J. Chem. Sci.* **2016**, *128*, 93.
[11] Y. Qi, H. Qi, J. Li, C. Lu, *J. Cryst. Growth* **2008**, *310*, 4221.
[12] Y. A. Attia, Y. M. A. Mohamed, *Appl. Organomet. Chem.* **2019**, *33*, e4757.
[13] Y. M. A. Mohamed, Y. A. Attia, E. J. Solum, *Res. Chem. Intermed.* **2018**, *44*, 7173.
[14] Y. A. Attia, C. V. Va'zquez, Y. M. A. Mohamed, *Res. Chem. Intermed.* **2017**, *43*, 203.
[15] Y. M. A. Mohamed, H. A. El Nazer, E. J. Solum, *Chem. Pap.* **2019**, *73*, 435.
[16] Y. A. Attia, *Mater. Express* **2016**, *6*, 211.
[17] S. S. A. D. M. Abadi, M. A. K. Zarchi, *New J. Chem.* **2017**, *41*, 10397.
[18] S. Behrouz, *J. Saudi Chem. Soc.* **2017**, *21*, 220.
[19] P. Movaheditabar, M. Javaherian, V. Nobakht, *Reac. Kinet. Mech. Catal.* **2017**, *122*, 217.
[20] G. Aridoss, K. K. Laali, *Eur. J. Org. Chem.* **2011**, *2011*, 6343.
[21] J. Safaei-Ghomi, S. Paymard-Samani, H. Shahbazi-Alavi, *J. Nanostruct.* **2018**, *8*, 383.
[22] J. A. Bladin, *Ber. Dtsch. Chem. Ges.* **1885**, *18*, 1544.
[23] I. Ugi, *Chem. Ber.* **1961**, *94*, 734.
[24] T. Kamiya, Y. Saito, JP Patent 7247031. Chem. Abstr. 1973, 78, 111331
[25] J. H. Toney, P. M. Fitzgerald, N. Grover-Sharma, S. H. Olson, W. J. May, J. G. Sundelof, D. E. Vanderwall, K. A. Cleary, S. K. Grant, J. K. Wu, D. L. Pompliano, G. G. Hammond, *Chem. Biol.* **1998**, *5*, 185.
[26] D. V. Dekhane, S. S. Pawar, S. Gupta, M. S. Shingare, C. R. Patil, S. N. Thore, *Bioorg. Med. Chem. Lett.* **2011**, *21*, 6527.
[27] C. N. S. S. P. Kumar, D. K. Parida, A. Santhoshi, A. K. Kota, B. Sridhar, V. J. Rao, *Med. Chem. Commun.* **2011**, *2*, 486.
[28] R. Romagnoli, P. G. Baraldi, M. K. Salvador, D. Preti, M. A. Tabrizi, A. Brancale, X. H. Fu, J. Li, S. Z. Zhang, E. Hamel, L. Chen, R. Bortolozzi, G. Basso, G. Viola, *J. Med. Chem.* **2011**, *55*, 475.
[29] A. L. Jackman, R. Kimbell, G. W. Aherne, L. Brunton, G. Jansen, T. C. Stephens, M. N. Smith, J. M. Wardleworth, F. T. Boyle, *Clin. Cancer Res.* **1997**, *3*, 911.
[30] K. Nagaraju, G. Lalitha, P. Singh, C. V. Rao, *Heterocycl. Commun.* **2017**, *5*, 365.
[31] S. Bahari, *Letters Org. Chem.* **2013**, *10*, 527.
[32] T. Jin, S. Kamijo, Y. Yamamoto, *Tetrahedron Lett.* **2004**, *45*, 9435.
[33] H. Sharghi, S. Ebrahimpourmoghaddam, M. M. Doroodmand, *J. Organomet. Chem.* **2013**, *738*, 41.
[34] M. Parveen, F. Ahmad, A. M. Malla, S. Azaz, *New J. Chem.* **2015**, *39*, 2028.
[35] D. Habibi, S. Heydari, A. Gil, M. Afsharfarnia, A. Faraji, R. Karamian, M. Asadbegy, *Appl. Organomet. Chem.* **2018**, *32*, e4005.
[36] A. Rostami-Vartooni, M. Alizadeh, M. Bagherzadeh, *Beilstein J. Nanotechnol.* **2015**, *6*, 2300.
[37] M. Nasrollahzadeh, M. Sajjadi, M. R. Tahsili, M. Shokouhimehr, R. S. Varma, *ACS Omega* **2019**, *4*, 8985.
[38] D. Habibi, N. Pakravan, A. Arabi, Z. Kaboudvand, *Appl. Organomet. Chem.* **2018**, *32*, e3988.
[39] R. Raghav, P. Aggarwal, S. Srivastava, *AIP Conf. Proceed.* **2016**, *1724*, 020078.
[40] S. M. Hosseini, I. A. Sarsari, P. Kameli, H. Salamati, *J. Alloys Compd.* **2015**, *640*, 408.
[41] P. A. Steiner, W. Gordy, *J. Molec. Spectr.* **1966**, *21*, 291.
[42] G. G. Archer, P. Wang, *J. Phys. Chem. Ref. Data Monogr.* **1990**, *19*, 371.
[43] S. Piiskop, S. Salmar, A. Tuulmets, A. Kuznetsov, J. Järv, *Ultrason. Sonochem.* **2013**, *20*, 1414.
[44] D. Habibi, M. Nasrollahzadeh, H. Sahebekhtiari, S. M. Sajadi, *Synlett* **2012**, *23*, 2795.
[45] D. Habibi, M. Nasrollahzadeh, *Synth. Commun.* **2012**, *42*, 2023.
[46] P. N. Gaponik, V. P. Karavai, Y. V. Grigor'ev, *Chem. Heterocycl. Comp.* **1985**, *21*, 1255.
[47] M. Ariannezhad, D. Habibi, S. Heydari, *Polyhedron* **2019**, *160*, 170.
[48] H. Naeimi, F. Kiani, *Ultrason. Sonochem.* **2015**, *27*, 408.

How to cite this article: Mohamed YMA, Attia YA. The influence of ultrasonic irradiation on catalytic performance of ZnO nanoparticles toward the synthesis of chiral 1-substituted-1*H*-tetrazolederivatives from α-amino acid ethyl esters. *Appl Organomet Chem*. 2020;e5758. https://doi.org/10.1002/aoc.5758